# DEVELOPMENT OF WELDABILITY ASSESSMENT AND UNDERSTANDING OF HOT CRACKING IN BOILER AND GAS TURBINE MATERIALS

KME-719





# DEVELOPMENT OF WELDABILITY ASSESSMENT AND UNDERSTANDING OF HOT CRACKING IN BOILER AND GAS TURBINE MATERIALS

KME-719

LARS NYBORG AND JOEL ANDERSSON

# **Preface**

The project has been performed within the framework of the materials technology research programme KME, Consortium materials technology for thermal energy processes, period 2014-2018. The consortium is at the forefront of developing material technology to create maximum efficiency for energy conversion of renewable fuels and waste. KME has its sights firmly set on continuing to raise the efficiency of long-term sustainable energy as well as ensuring international industrial competitiveness.

KME was established 1997 and is a multi-cliental group of companies over the entire value chain, including stakeholders from the material producers, manufacturers of systems and components for energy conversion and energy industry (utilities), that are interested in materials technology research. In the current programme stage, eight industrial companies and 14 energy companies participate in the consortium. The consortium is managed by Energiforsk.

The programme shall contribute to increasing knowledge within materials technology and process technology development to forward the development of thermal energy processes for efficient utilisation of renewable fuels and waste in power and heat production. The KME goals are to bring about cost-effective materials solutions for improved fuel flexibility, improved operating flexibility, increased availability and power production with low environmental impact.

KME's activities are characterised by long term industry and demand driven research and constitutes an important part of the effort to promote the development of new energy technology with the aim to create value and an economic, environmentally friendly and long term sustainable energy society.

The industry has participated in the project through own investment (60 %) and the Swedish Energy Agency has financed the academic partners (40 %).

Bertil Wahlund, Energiforsk



## **Abstract**

The aim of the project is to bring an improved understanding of weldability with a specific focus on hot cracking of alloys used in temperature applications. The alloys investigated were austenitic stainless steel 314, which is being used in the boiler industry, as well as Ni-based superalloys such as the cast Alloy 718, wrought and cast ATI 718Plus which are being used in aeroengine applications. A state-of-the art Varestraint weldability test method was developed during a previous KME research project and has been used for testing in the current project.

It was found that the pre-weld heat treatment condition significantly influences the hot cracking susceptibility of the Ni-based superalloys. Generally, by increasing heat treatment temperature and the soak time, the extent of the cracking increased in the weld heat affected zone. Moreover, testing of the austentic stainless steel showed that the welding parametres also play an important role relative to the cracking and the scatter of the results.

The report includes the weldability testing data for the different alloys together with report of the general microstructure of the base metal, heat treatments and welded zones with an overview of the main factors influencing the cracking susceptibility.



# Sammanfattning

Syftet med projektet var att öka förståelsen för mekanismer gällande svetssprickor och specifikt varmsprickor. Materialet i fokus har varit austenitiskt rostfritt stål och nickelbaserade material där den sistnämnda gruppen inkluderat både gjutgods och plåt. Varestrainprovning har använts som metod i att undersöka sprickkänsligheten av de olika materialen och att tillsammans med omfattande materialkaraktärisering försöka få en fördjupad förståelse om de avgörande sprickmekanismerna.

Projektet (KME 719) har utförts i samarbete mellan Chalmers Tekniska Högskola och GKN Aerospace Sweden AB. I referensgruppen så har även panntillverkarna Sumitomo och Dong Energy varit inkluderade.

Svetsbarheten av tre nickelbaserade superlegeringar benämnda gjutet Alloy 718, gjutet ATI 718Plus och plåt ATI 718Plus har undersökts och presenterats vid "International Institute of Welding (IIW)" årliga sammanträden under 2016 och 2017 samt vid konferensen "Superalloys 718 & Derivatives" 2018. Gällande det austenitiska rostfria stålet 314 så har två stycken publikationer presenterats på konferensen "Swedish Manufacturing Symposium conference (SPS)" under 2016 respektive 2018.

Undersökningar gällande inverkan av värmebehandling innan svets med avseende på varmsprickor hos gjutet 718 och ATI 718Plus samt plåt för ATI 718Plus har genomförts. Resultatet visade att värmebehandling vid högre temperatur och längre hålltid gav en ökad mängd sprickor i den värmepåverkade zonen i jämförelse med lägre värmebehandlingstemperatur och hålltid. Gällande det austenitiska rostfria stålet 314 så har en omfattande försöksplanering utförts med avsikten att undersöka svetsparamtrars inverkan på varmsprickor. De svetsparametrar som gav minst andel svetssprickor identifierades och finns tillgängliga tillsammans med ytterligare svetsbarhetsdata i slutrapporten.



# **Summary**

The aim of the project was to bring an improved understanding of weld-cracking mechanisms important for hot cracking. The materials involved were austenitic stainless steels and Ni-based superalloys where the last material group was present in both wrought and cast form. The testing procedure that was used was the Varestraint weldability testing method in order to assess hot cracking susceptibility of the different alloys together with in depth microstructural characterization to provide insight into the ongoing mechanisms.

The project (KME 719) has been carried out as a cooperation between Chalmers University of Technology and GKN Aerospace Sweden AB. In the reference group, participants from the boiler industry, Sumitomo and Dong Energy, were also included. The weldability of three Ni-based superalloys cast Alloy 718, cast ATI 718Plus and wrought ATI 718Plus have been evaluated and presented at the International Institute of Welding (IIW) annual assemblies in 2016 and 2017 and at the Superalloys 718 & Derivatives Conference 2018. This led to 2 articles in peer reviewed journals and one conference proceeding. Relative to the austentic stainless 314, two publications were presented at the Swedish Manufacturing Symposium conference (SPS) in 2016 and 2018.

The effect of the pre-weld heat treatments on the hot cracking susceptibility of cast Alloy 718, cast ATI 718Plus and wrought 718Plus were investigated. It was found that the heat treatments at higher temperatures and longer dwell times increased the cracking susceptibility in the weld heat affected zone. Regarding the austenitic stainless steel 314, a relatively large DOE was conducted to study the influence of the welding parametres on the weld cracking susceptibility. The weld parameters exhibiting the lowest extent of cracking and the least amount of variability were also suggested. Additional weldability data is also included in this report.



# **List of content**

1	Intro	duction	9
	1.1	Background	9
	1.2	Description of the research field	g
	1.3	Research tasks	g
	1.4	Goals	9
	1.5	Project organisation	10
2	Expe	rimental	11
	2.1	CAST ALLOY 718	11
	2.2	CAST 718 PLUS	12
	2.3	WROUGTH 718 PLUS	13
	2.4	AUSTENITIC STAINLESS STEEL 314	13
3	Resu	lts	15
	3.1	CAST ALLOY 718	15
	3.2	CAST 718 PLUS	18
	3.3	WROUGHT 718 PLUS	20
	3.4	AUSTENITIC STAINLESS STEEL 314	25
4	Anal	ysis of the results	30
	4.1	CAST ALLOY 718	30
	4.2	COMPARISON OF CAST ALLOY 718 AND 718 PLUS	32
	4.3	WROUGTH 718 PLUS	33
	4.4	Austenitic stainless steel 314	34
5	Conc	lusions	35
	5.1	CAST ALLOY 718	35
	5.2	CAST 718 PLUS AND COMAPRISON WITH CAST ALLOY 718	35
	5.3	Wrougth 718 plus	35
	5.4	AUSTENITIC STAINLESS STEEL 314	35
6	Goal	fulfilment	37
7	Sugg	estions for future research work	38
8	Litera	ature references	39
9	Puhli	ications	40



# 1 Introduction

### 1.1 BACKGROUND

There are numerous welds in boiler systems and gas turbines. Also, as steam and gas temperatures are increased, it will affect the materials used in the boiler plants and turbines. Some materials will no longer be able to withstand the higher temperature which in turn introduces new type of materials with limited knowledge regarding its weldability or resitance towards cracking during welding. The procedure in which weldability is being determined is for many reasons not always an easy target. There are many parametres which come to play when assessing a material's resistance to cracking where material chemistry, condition (e.g. cast or wrougth, grain size etc), and welding parameres are important just of mention a few. The proposed project is two-fold in tis content and specifically aims to investigate the weldability of materials that are of interest both to the boiler (superheater and reheater tubes) and gas turbine (turbine casings) manufacturers, secondaly to develop further understanding and capability to perform the actual weldability assessment. Materials that are to be included in the investigation are austenitic steels and superalloys; 314, Cast Alloy 718, Cast ATI 718 Plus and wrought ATI 718 Plus. The material selection for this project have been discussed with Sumitomo SHI FW and GKN Aerospace who both partecipate in the project reference group. The actual weldability assessment was carried out using a specially designed and state-of-the-art-Varestraint weldability testing.

### 1.2 DESCRIPTION OF THE RESEARCH FIELD

The research field has mainly covered precipitation hardening Ni-based superalloys (Cast Alloy 718, Cast ATI 718 Plus and wrought ATI 718 Plus) and austenitic stainless steel 314, which have been tested by the state-of-art-Varestraint testing equipment and examined from a metallurgical standpoint. Part of the research is described in the articles in the publication list at the end of the report.

### 1.3 RESEARCH TASKS

The aim of the project KME 719 is to investigate and develop further understanding of hot cracking mechanism as well as how to assess the susceptibility towards these cracks in a reliable way. The project also aims to recommend and make guidance to boiler plant manufacturers and other relevant industries in terms on how to minimize the type of problems which are associated with hot cracking. These recommendations could aid in design and manufacturing of new plants as well as repair of worn out parts. Primarly, the effect of heat treatments and welding parametres on hot cracking susceptibility have been investigated. This has been investigated by weldability testing using Varestraint and material characterization.

### 1.4 GOALS

The overall goal of the project is to increase the overall understanding of hot cracking mechanism as well as to develop weldability testing capability towards hot cracking in a reliable way. This aim has been limited to the following objectives:



### Academic goals

To accomplish a licentiate engineer To develop a unified theory for hot cracking To develop a testing rationale for hot cracking

### **Industrial** goals

To generate weldability test data on materials relevant to the boiler industry
To recommend materials and parametres for improved weldability
To establish a testing methodology that can be used for assessing weldability with respect to hot cracking susceptibility

### 1.5 PROJECT ORGANISATION

The project is based on collaboration in between Chalmers University of Technology and GKN Aerospace Sweden AB. Sumitomo SHI and Örsted have also participated in the project.

The industrial partner of the project has been GKN Aerospace Sweden AB. The in-kind contribution from GKN is 5612750 SEK.

The Swedish Energy Agency has supported to project with 3500000 SEK and this funding has been assigned to the academic partner Chalmers University of Technology. The share of public funding has hence been 38.4%.

The engaged staff in the project organization comprised of a project management group led by Dr. Geraldine Puyoo at GKN Aerospace Sweden AB (Geraldine Puyoo, Bengt Pettersson and Johan Ockborn) where also members from Chalmers University of Technology (Sukhdeep Singh, PhD student, Joel Andersson and Lars Nyborg, supervisors) have been included. Project management group meetings have been held once per month to review the monthly deliverables as well as other technical apects. Supervision meetings have been held every second week separately to the project management group meetings. The project has also been organised with a reference group with meetings once every second month including the representation by GKN Aerospace Sweden (Dr. Geraldine Puyoo), Sumitomo SHI (Jouni Mahanen), Dong Energy/Örsted (Soren Jensen) and Chalmers University of Technology (Sukhdeep Sing and Joel Andersson or Lars Nyborg).



# 2 Experimental

### 2.1 CAST ALLOY 718

The alloy composition is presented in Table 2.

Table 1. Composition of Alloy 718 in wt%

Ni	Fe	Cr	N	M	Ti	Al	M	Co	С	Si	С	S	P	В	V	W
			b	О			n		u							
52.	Ва	18.	5.3	2.9	0.9	0.4	0.0	0.0	0.0	0.0	0.0	0.0	0.00	0.0	<0.	<0.
98	1.	11	1	8	9	2	3	7	1	7	5	02	09	03	1	01

The complete details of the HIP conditions are represented in Table 3.

Table 2. HIP treatments steps for cast Alloy 718

Condition	HIP at 100 MPa	Post-HIP in Vacuum	Solution heat treatment
HIP-1120 [8]	1120°C/4h	1050°C/1h + FC to 650°C in 1h	950°C/1h + AC
HIP-1190 [9,10]	1190°C/4h	870/10h + FC to 650°C in 1h	950°C/1h + AC

FC=furnace cooling, AC=air cooling

For each condition, ten cast plates were received from the supplier with approximate dimensions of 300x60x12 mm. Each plate was electric discharge machined into six small test samples with approximate dimensions of 150x60x3.3 mm. A state of art Varestraint weldability testing machine was used at test radii varying from 20 to 200 mm, corresponding to strain levels of 0.8, 1.1, 1.6, 2.1, 2.7, 3.3, 3.9 and 8.2%. The test set up is described elsewhere [12]. The strain ( $\epsilon$ ) is given by the following equation:

$$\varepsilon = \frac{t}{2R} \tag{eq.1}$$

Where t is the thickness of the plate (3.3 mm) and R is the die radius. For each die radii and condition a total of 7 plates were tested. The welding and testing parameters are based from a DOE study which produced the lowest average total crack length and lowest standard deviation among different settings [12]. The gas tungsten arc welding (GTAW) parameters are presented in Table 4.

Table 3. Welding parameters for GTAW during longitudinal Varestraint testing [12]. Argon gas purity of 99.99%

Welding Speed (mm/s)	Stroke Rate (mm/s)	Arc length (mm)	Welding Current (A)	Ar gas flow (l/min)
1	10	2	70	15

The surfaces of the Varestraint tested samples were manually polished by using abrasive paper Carbimet™ to remove any oxide layer and crack measurements were conducted by using stereo microscope at 57x magnification. Samples were cut and mounted using standard procedures and subsequently etched by Kalling′s 2 (2g CuCl₂, 49mL HCl, 40-80 mL ethanol) and etchant 13 (10g oxalic acid, 100mL water). Weld bead dimensions were measured on cross-sections obtained from the area experiencing maximum amount of bending, at a distance of 15 mm from the end of the weld. Microstructural evaluation was conducted by optical microscopy and scanning electron microscopy (LEO 1550 FEG-SEM with Oxford Electron Dispersive X-ray Spectroscopy).



### 2.2 CAST 718 PLUS

The composition in wt% of cast ATI® 718PlusTM is presented in Table 5. Differential Scanning Calorimetry (DSC) was performed by Netzsch-STA 409 PC Luxx simultaneous DSC-TG equipment using heating and cooling rates of 20°C/min for solidification sequences and comparison was made by simulation results obtained by JMatPro v8. The selected pseudo-HIP treatments were 1120°C, 1160°C, 1190°C for 4h and 1120°C and 1190°C for 24h dwell time followed by water quenching in order to avoid any precipitation of  $\gamma'$ . These five conditions were tested in reference to the as cast condition.

Table 4. Composition of wrought ATI® 718 PlusTM, cast ATI® 718 PlusTM and cast Alloy 718

Element (wt %)	Wrought ATI® 718PlusTM	Cast ATI® 718PlusTM	Cast Alloy 718
Ni	Bal.	Bal.	52.98
Cr	18	20.5	18.11
Fe	10	9.7	Bal.
Co	9	8.3	0.07
Nb	5.45	6.3	5.31
Mo	2.8	2.7	2.98
Al	1.45	1.5	0.42
Ti	0.7	0.8	0.99
C	0.02	0.05	0.05
W	1	1	0.01
Mn	-	0.01	0.03
Cu	-	0.1	0.01
Si	-	0.03	0.07
P	0.007	0.008	0.009
В	0.004	0.005	0.03

Three test plates for each condition were tested using longitudinal Varestraint weldability testing at augmented strain levels of 1.1%, 1.6%, 2.1% and 2.7%. The test set up, available in reference [10], and welding conditions are the same as for the previous study of cast Alloy 718 [8]. The welding parameters are summarised in Table 6.

Table 5. Parameters used for Varestraint weldability testing using gas tungsten arc welding. Ar gas purity of 99.99%

Welding Speed (mm/s)	Stroke Rate (mm/s)	Welding Current (A)	Arc length (mm)	Ar gas flow (l/min)
1	10	70	2	15

After testing, the plate surfaces were manually polished by fine abrasive paper to remove any oxide layer. Cracks were measured by stereo microscope at x57 magnification. Volume fraction of secondary precipitates were carried out by manual point count according to ASTM E562 [11]. Grain size measurements were conducted on two samples from each test plate (totally 144 samples). Macroetching was conducted by using the etching solution of HCL with mean concentration of 90%, 10% HNO3, 120 g/L FeCl3 powder heated to about 50°C. Varestraint tested samples as well as samples for determining the grain size were etched electrolytically by oxalic acid at 5V and varying times and characterized by optical as well as scanning electron microscopy (LEO 1550 FEG-SEM with Oxford Electron Dispersive X-ray Spectroscopy).



### 2.3 WROUGTH 718 PLUS

Composition of the wrought ATI 718Plus® used in the current study is presented in Table 7.

Table 6. Composition of ATI 718Plus® in wt%

Ni	Cr	Fe	Со	Мо	Al	Ti	Nb	С	В	Р	S	W
Bal.	17.86	9.59	8.97	2.70	1.49	0.76	5.49	0.024	0.004	0.010	0.003	0.99

The welding and testing parameters for longitudinal Varestraint testing are shown in Table 8. Augmented strain levels for the test were between 2.1-4.3%. Support plates were tack-welded on the backside of the test plates to avoid hinging during bending.

Table 7. Welding parameters for GTAW (Gas Tungsten Arc Welding) Varestraint testing

Welding Speed	Welding Speed Stroke Rate		Ar Gas Flow	
2 mm/s	16 mm/s	85 A	18 l/min	

After testing, plate surfaces were cleaned to remove any oxide layer and crack measurements were conducted by using a stereo microscope. Conventional metallographic procedures followed to prepare the samples and etching was carried out electrolytically by using oxalic acid as well as Kalling's No. 2 etchant for microscopic evaluation. Grain size measurements were conducted according to ASTM E112 standard [11] and micro-Vickers test (0.5 kgf/HV 0.5) for hardness measurements was used. High resolution characterization was conducted by the use of a LEO 1550 field-emission gun scanning electron microscope (FEG-SEM) equipped with Energy Dispersive X-ray Spectroscopy (EDS).

### 2.4 AUSTENITIC STAINLESS STEEL 314

The chemical composition in wt % of the 314 austenitic stainless steel can be seen in Table 9.

Table 8. Chemical composition of the austenitic stainless steel 314 in wt%

С	Si	Mn	P	S	Cr	Mo	Ni	N	Ti
0.057	1.91	1.42	0.024	0.0008	24.27	0.45	19.04	0.030	0.057

Test plates with dimensions of  $150 \times 50$  mm were cut out from a large sheet with 5 mm in thickness and tested in the solution heat treated condition ( $1050^{\circ}$ C followed by air cooling). Three different sets of welding parameters were used with varying current and welding speed while maintaining constant arc length of 3 mm and the same heat input as per Table 10. Argon shielding gas of 15 l/min was used to protect the welds from oxidation.

Table 9. GTAW (gas tungsten arc welding) test parameters used Varestraint testing

	Current	Voltage	Speed (mm/min)	Heat Input (KJ/mm)
a	100	10	70	0.8
b	140	10	100	0.8
c	180	10	130	0.8



The three test conditions are hereafter referred to as 100\_70, 140\_100 and 180\_130, respectively. Bead on plate welds were performed by longitudinal Varestraint weldability testing equipment, Figure 1. Figure 2 discloses the details of the test set up. Test plates were positioned on top of the die mandrel. Once the welding reached a steady state condition, bending was performed with the help of two support plates in order to have uniform bending. Testing was conducted at a fixed augmented strain level of 5% and by using a stroke rate of 1 mm/s. Three test plates were tested for each set of welding parameter. After testing, weld surfaces were cleaned to remove any oxide layers by the use of fine grinding paper. Crack measurements of the top surface of respective specimen were conducted using a stereo microscope. Ferrite measurements in the base metal and weld metal were carried out by using a Feritscope. Sample preparation followed the conventional procedures of manual cutting, mounting, grinding and polishing steps. Samples were etched electrolytically by oxalic acid solution. The samples were overetched in order to reveal the grain boundaries for grain size measurements. Microstructural investigation was conducted by optical light microscopy. Hardness measurements were conducted by Vickers microhardness test using HV0.5 load.



# 3 Results

### 3.1 CAST ALLOY 718

This study investigates the effect of two different HIP (Hot Isostatic Pressing) treatments in reference to the as cast condition by Varestraint testing. The HIP treatments are presented in the following Table 11.

Table 101. HIP treatments steps for cast Alloy 718

Condition	HIP at 100 MPa	Post-HIP in Vacuum	Solution heat treatment
HIP-1120 [8]	1120°C/4h	1050°C/1h + FC to 650°C in 1h	950°C/1h + AC
HIP-1190 [9,10]	1190°C/4h	870/10h + FC to 650°C in 1h	950°C/1h + AC

Test parametres are presented in Table 12.

Table 111. Welding parametres for gas tungsten arc welding during longitudinal Varestraint testing

Welding Speed	Stroke Rate	Arc length	Welding Current (A)	Ar gas flow
(mm/s)	(mm/s)	(mm)		(l/min)
1	10	2	70	15

Figure 1 shows the weld grain structures of the three conditions. The three sections are taken from plates tested at 2.7% augmented strain. It can be seen different weld grains structures occurred, with few and small equiaxed grains in the as cast condition and prevantly columnar grains in the HIP conditions.



Figure 1. Weld grain structure and cracking in plates tested at 2.7% augmented strain.

Weld bead dimensions from plates tested at 4% augmented strain are disclosed in Table 13. Weld cross sections can be seen in Figure 2.

Table 112. Weld bead dimensions taken by averaging measurements of three plates from each condition

Condition	Depth (mm)	Width (mm)	Undercut (mm)	D/W
As Cast	4.03±0.06	7.03±0.12	0.4±0	0.57±0.02



HIP-1120	4.5±0.17	7.43±0.21	0.67±0.25	0.61±0.01	
HIP-1190	3.93±0.40	7.43±0.21	0.31±0.44	0.53±0.05	

It can be seen that the while width values were within tolerances, the penetration depths had major variations and overall weld shapes were different taking into consideration the undercut values.

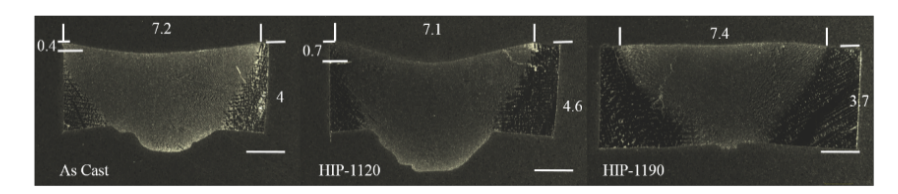


Figure 2. Weld cross sections from plates tested at 4% augmented strain.

As to be expected, the as cast condition showed high amount of segregation, with 3.7 volume fraction (Vv) of secondary precipitates (Table 4), in the interdendritic regions from Nb rich consituents (Laves and NbC). A detailed high resolution image of the Laves eutectic can be seen in Figure 3.

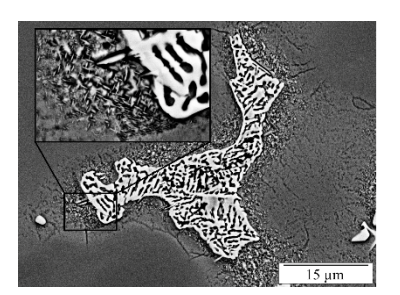


Figure 3. Backscattered SEM image of Laves phase with eutectic morphology surrounded small precipitates that resemble  $\gamma^{\prime\prime}$ .

In the HIP treated conditions, the amount of segregation is much lower in comparison to as cast condition but with slight difference between HIP-1120 and HIP-1190. The evolution of the secondary phase precipitates in HIP treatments can be seen in Figure 4. Adjacent to them small amounts of delta phase precipitation was seen to occur.

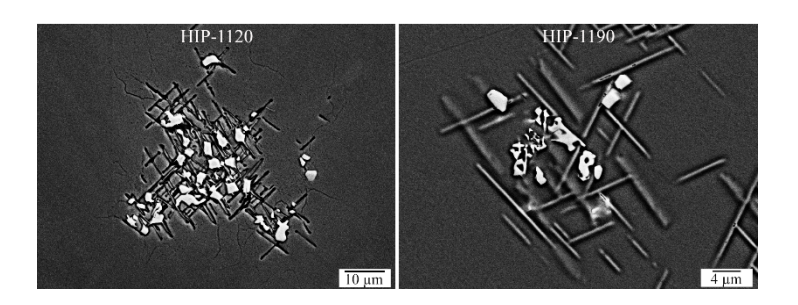


Figure 4. Backscattered images showing evolution of segregating phases in the HIP conditions.



Grain size measurements from Table 14 reveal the typical large grain size of cast materials. As cast has the lowest average grain size of 1.7 mm, followed by HIP-1120 (2.6 mm) and HIP-1190 (3.3 mm), respectively. No significant difference in base metal hardness was observed.

Table 113. Volume fraction of secondary precipitates, grain size measurements and base metal hardness

Condition	Vv (%)	GS (mm)	HV
As Cast	3.7±0.6	$1.7 \pm 0.1$	260±20
HIP-1120	1.7±0.1	2.6±0.3	220±30
HIP-1190	1.3±0	3.3±0.3	210±20

Heat affected zone liquation cracking in the as cast condition was associated with liquation of the Laves eutectic, as can be visualized in Figure 5. On the other hand, in the HIP conditions, no large liquated Laves clusters were seen. The cracking followed along grain boundaries and was characterized by presence of eutectic constituents.

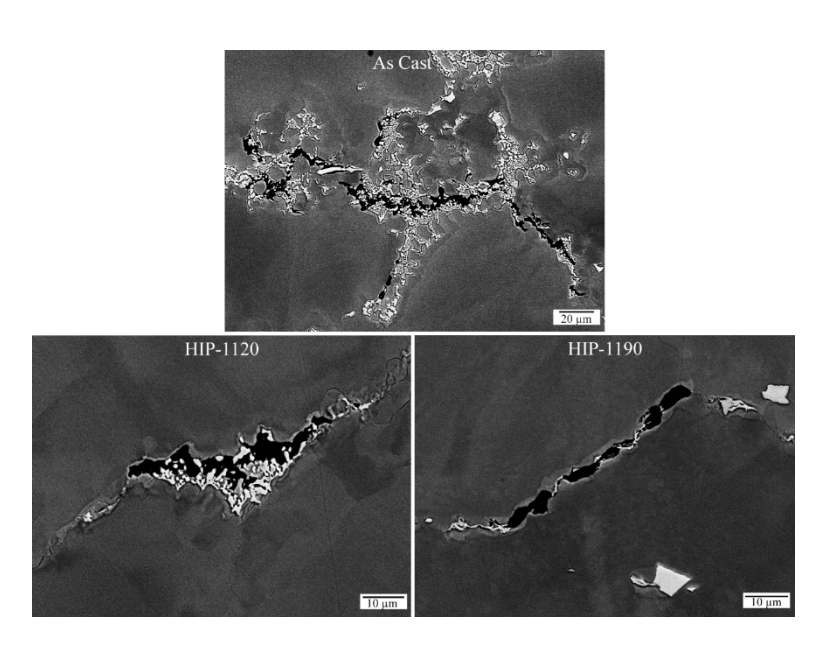


Figure 5. Backscattered SEM images showing the HAZ liquation cracking.

The average total crack length (Avg. TCL) values against augmented strain for fusion zone (FZ) graph is plotted in Figure 6.



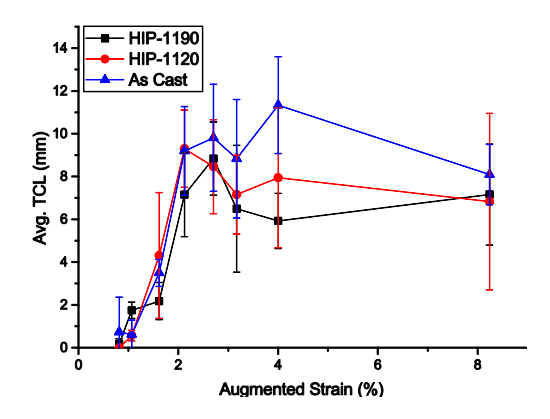


Figure 6. FZ cracking response with standard deviations for the as cast, HIP-1120 and HIP-1190 conditions.

Cracking related to the HAZ liquation is shown in Figure 7.

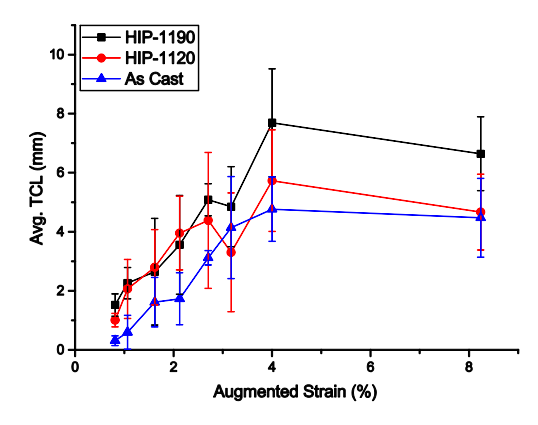


Figure 7. HAZ liquation cracking response with standard deviations for the as cast, HIP-1120 and HIP-1190 conditions.

Out of the original 168 test plates, 10 were excluded as the test did not proceed correctly. Rejection criteria were the S-shaped welds indicating the robot did not weld in straight line, and the tungsten electron tip hit the plate. Therefore, a few data points are missing in the plot. These points belong to three samples each for the as cast and HIP-1190 condition at 2.7% augmented strain and two samples each for the as cast and HIP-1120 at 3.2% augmented strain.

### 3.2 CAST 718 PLUS

This study investigates the effect of different Pseudo-HIP treatments at  $1120^{\circ}\text{C/4h}$ ,  $1160^{\circ}\text{C/4h}$ ,  $1190^{\circ}\text{C/4h}$  and  $1190^{\circ}\text{C/24h}$  in reference to the as cast condition. Test parameters were same as for the previous study.

The volume fraction of secondary precipitates reduced significantly after Pseudo-HIP at  $1120^{\circ}$ C/4h, see Table 3. Other heat treatments at higher temperature/longer dwell times had a lower influence reaching 0.2% at  $1190^{\circ}$ C. Hardness in the heat treated conditions dropped to 170-180HV from the 375 HV in the as cast condition. As per values in Table 15, grain growth did not occur after the heat treatments.



Table 114. Volume fraction of secondary precipitates, grain size measurements and base metal hardness

	As Cast	1120°C/4h	1120°C/24h	1160°C/4h	1190°C/4h	1190°C/24h
Vv (%)	3.2±1.8	0.7±0.6	0.4±0.2	0.3±0.1	0.2±0.1	0.2±0.1
HV	375±15	170±0	180±0	170±5	170±0	180±5
GS	2.3±0.5	2.2±0.5	2.4±0.5	2.3±0.4	1.7±0.4	2.5±0.6
(mm)						

Figure 8 shows the grain structure in the as cast condition with variation in grain size on the two sides of the weld bead. Figure 9 represents a weld corss-section from the as cast condition.



Figure 8. Varestraint test plate showing difference in grain size on two sides of the weld bead.

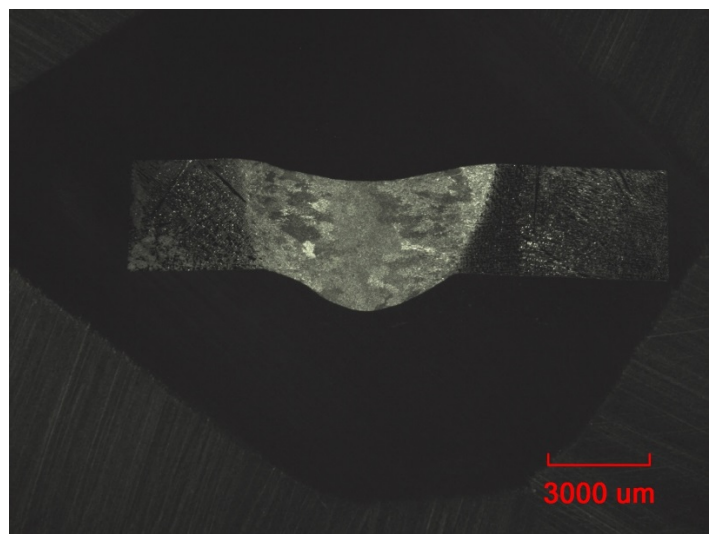


Figure 9. Weld cross section for the as cast condition.

Fusion zone cracking response is shown in terms of average total crack length in Figure 10. It can be seen that no difference in solidification cracking response was found.



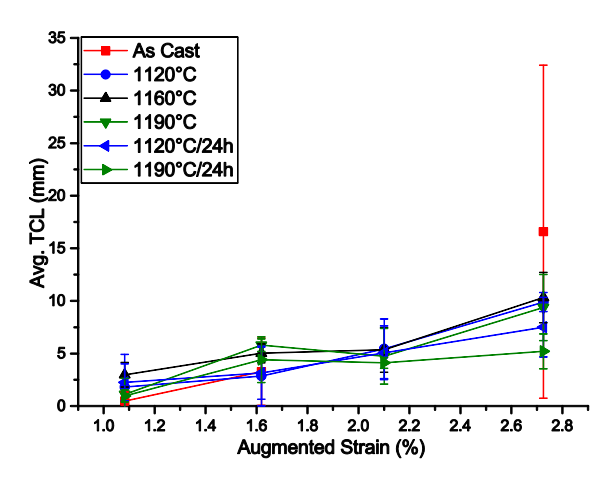


Figure 10. FZ cracking response with standard deviations for the different conditions.

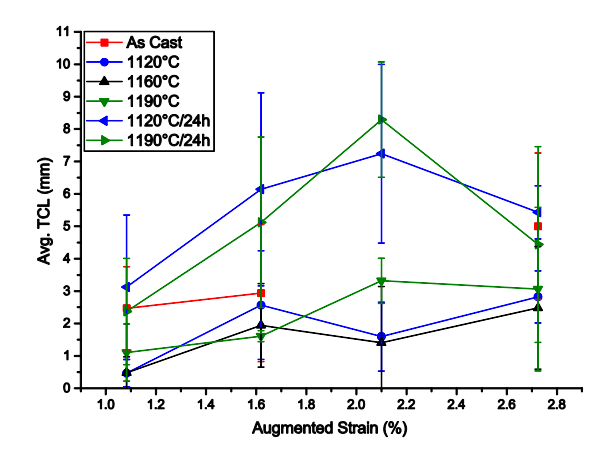


Figure 11. HAZ cracking response for the different conditions.

Cracking response in the heat affected zone is presented in Figure 11. Although, being very scattered values, no clear difference can be seen for the 4 h dwell heat treatment. However, average total crack length increased with longer homogenization times.

### 3.3 WROUGHT 718 PLUS

The effect of eta phase on the weldability of wrougth 718 Plus was investigated in this study. High fraction of eta precipitation was obtained by subjecting the alloy to heat treatment at 950°C/15h. The weldability of this condition was compared to that of 950°C/1h by Varestraint testing. Test paremetres are presented in Table 16.

Table 115 Welding parameters for GTAW (Gas Tungsten Arc Welding) Varestraint testing

Welding Speed	Stroke Rate	Welding Current	Ar Gas Flow
2 mm/s	16 mm/s	85 A	18 l/min

Significant amounts of eta phase in the form of long and thick plate-like precipitates are present both inter- and intragranularly in Figure 12 b). On the other hand, the short dwell heat treatment at 950°C/1 h produced a small amount of precipitates mainly along the grain boundaries, Figure 12 a).



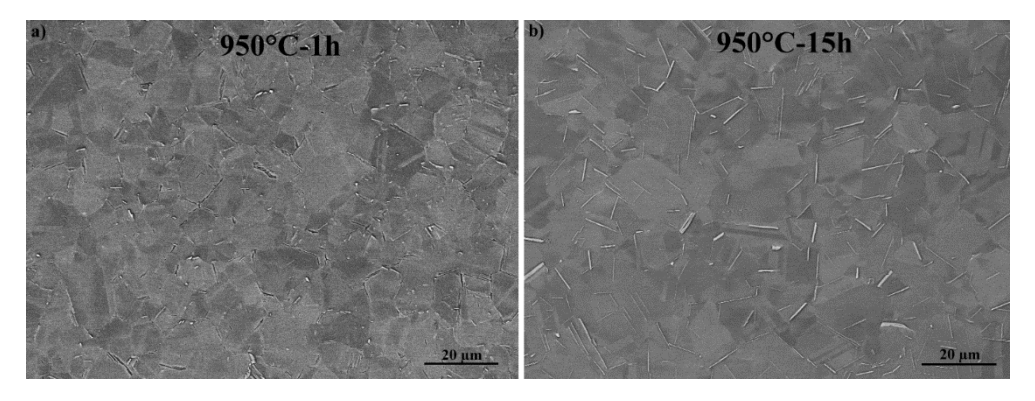


Figure 12. SEM images comparing the precipitation of eta phase in the a) 950°C/1 h and b) 950°C/15 h heat-treated materials.

Crack measurements after longitudinal Varestraint testing of the  $950^{\circ}$ C/15 h condition are presented in Figure 13. These measurements include both cracking occurring in the fusion zone (FZ) and heat-affected zone (HAZ) and are compared to the data relative to  $950^{\circ}$ C/1 h condition, obtained from a previous study conducted by Jacobsson et al. [9]. The comparison in Figure 13 clearly discloses an increased cracking susceptibility for  $950^{\circ}$ C/15 h condition over  $950^{\circ}$ C/16 h condition.

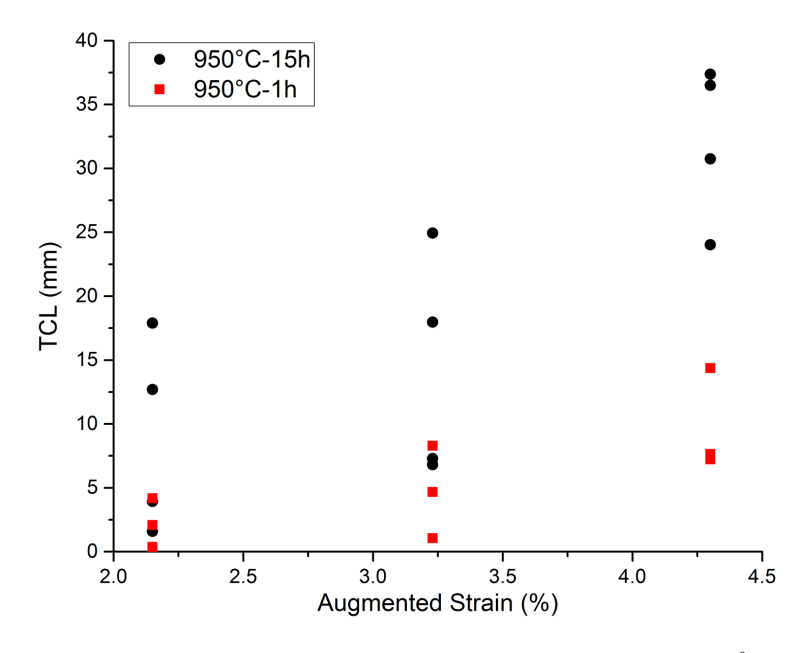


Figure 13. Varestraint testing results comparing two conditions of wrought ATI 718Plus $^{\circ}$  heat treated at 950 $^{\circ}$ C/1 h [9] and 950 $^{\circ}$ C/15 h.

Hardness profiles across the weld cross-sections are plotted in Figure 14. Base metal hardness of the 950°C/1 h heat-treated condition was about 380 HV, in comparison to about 340 HV in the 950°C/15 h condition. Hardness values decreased in the HAZ following similar trend and reached the lowest values of about 250 HV in the FZ.



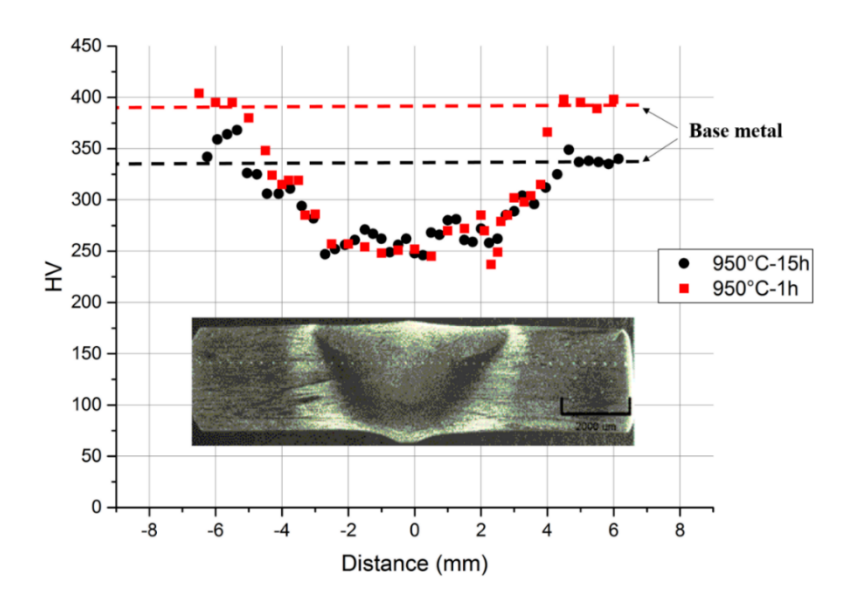


Figure 14. Micro-hardness profiles across the weld cross-sections in the two heat-treatment conditions.

Regarding the grain size, although being similar in the two heat-treated conditions as can be seen in Table 17, significant grain growth occurred in the HAZ of 950°C/1 h condition upon welding, leading to about three times larger grain size than the starting condition.

Table 116. Base metal and HAZ grain size for the two heat-treated conditions

	BM Grain Size (μm)	HAZ Grain Size (μm)					
950°C/1 h	8.3	30					
950°C/15 h	7.8	9.6					

Grain boundaries liquated in the PMZ (Partially Melted Zone) of the 950°C/1 h condition. Almost complete dissolution of eta phase occurred in the region adjacent to the fusion line with residual traces of eutectic constituents along the grain boundaries. Constitutional liquation of the primary NbC also occurred in this region. A representative microstructural micrograph of the highly liquated (HL) region is shown in Figure 15.



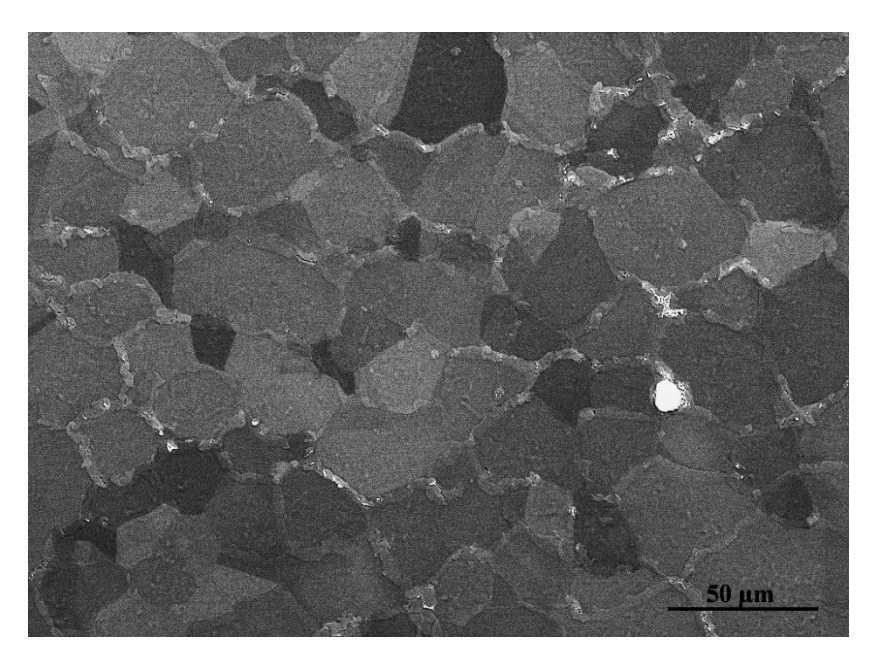


Figure 15. SEM image illustrating grain boundary liquation in the PMZ of the condition subjected to  $950^{\circ}$ C/1 h heat treatment.

Further into the PMZ, no liquation was observed for the carbides nor any complete dissolution of the eta phase as shown in the highlighted region in Figure 16. The cracking occurring in this region was associated with the eutectic-like structure as also visible from Figure 16.

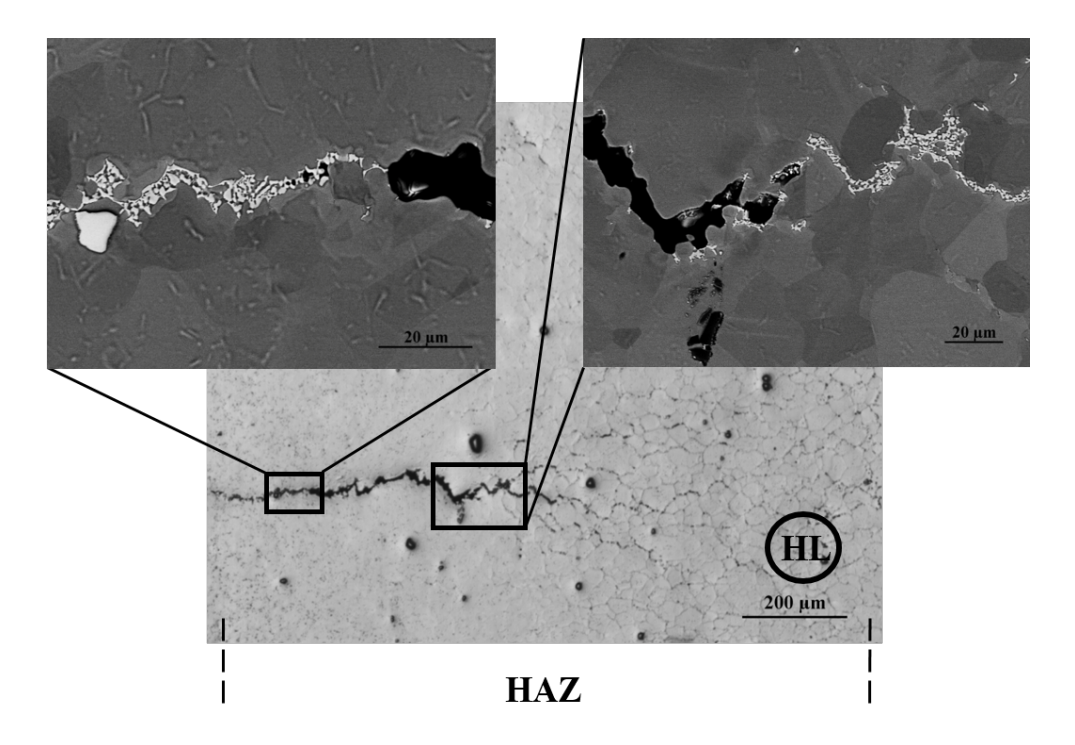


Figure 16. Optical and SEM images showing microstructure of the HAZ and cracking occurring in the 950°C/1 h condition.



Grain boundary liquation occurred to a higher extent in the PMZ of the 950°C/15 h in relation to 950°C/1 h condition, as visible in Figure 17. The bright phases in the backscattered electron SEM image exhibit traces of liquation products.

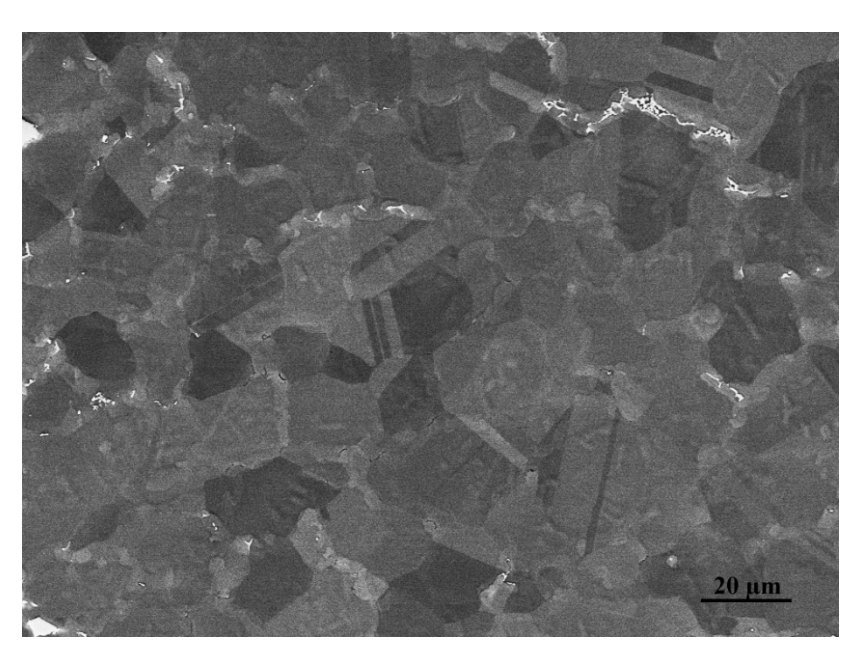


Figure 17. SEM image representing grain boundary liquation in the PMZ of the 950°C/15 h heat-treatment condition.

Constitutional liquation of NbC also occurred in the 950°C/15 h condition adjacent to the fusion line, and cracks in the PMZ connected to the fusion zone revealed the presence of gamma-eutectic constituents, Figure 18. Figure 18 reveals a number of cracks occurring further in the PMZ. These cracks, however, did not show any presence of eutectic phases in the backscattered electron SEM images nor any significant enrichment of Nb around the cracked area.



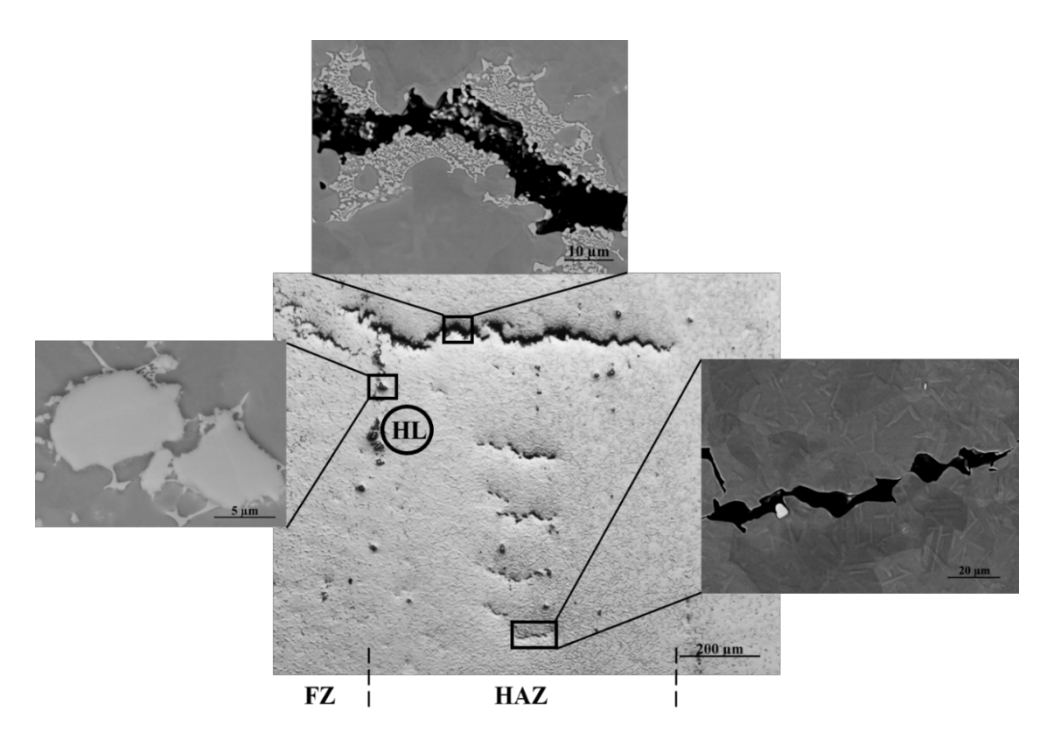


Figure 18. Optical and SEM images showing microstructure of HAZ and cracking occurring in the 950°C/15 h condition.

### 3.4 AUSTENITIC STAINLESS STEEL 314

This study investigates the effect of welding parametres on solidification cracking of austenitic stainless steel 314. Test parametres are presented in Table 8.

Table 17. Test parametres for Varestraint testing.

	Amperage	Voltage	Speed (mm/min)	Heat Input (KJ/mm)
а	100	10	70	0.8
b	140	10	100	0.8
С	180	10	130	0.8

Crack measurements from each test plate are represented in terms of TCL (Total crack length) in Figure 19. It can be seen the welding condition described as 100\_70, where 100 is the amperage and 70 is the welding speed, overall disclosed the lowest amount of cracking of about 25 mm with similar values between the three plates. Increasing amperage and welding speed (180\_130) resulted in incre condition with intermediate amperage and speed, 140\_100, exhibited a relatively high scatter with minimum value of 23 mm and maximum 41 mm.



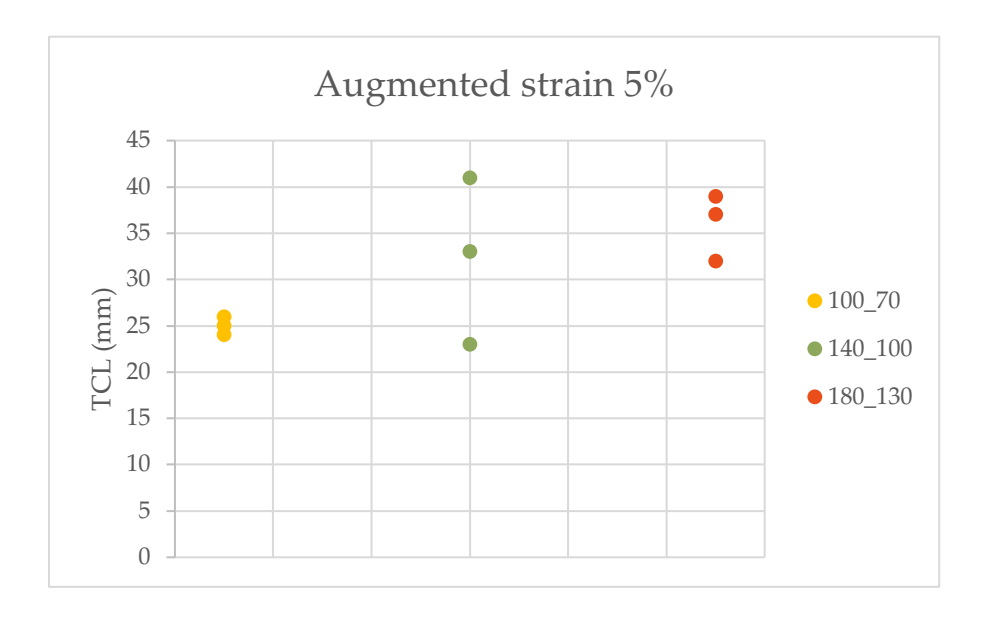


Figure 19. Total crack length values for the solidification cracks at 5% augmented strain.

Figure 20 represents the weld profiles with top and transversal views. It can be seen that while the weld penetration was similar for the three test parameters of about 2 mm, the width increased significantly from 6.6 mm for the 100\_70 to 10.2 mm for the 180\_130 and intermediate value of 8.7 mm for the 180\_130. It is also interesting to see the morphology of the cracking, with centerline cracks for the 100\_70 and 140\_100, whilst the solidification cracks appeared to be transversal to the welding direction in 180\_130. Another interesting fact is that cracking started in earlier stage for the 180\_130 as indicated the dash line.



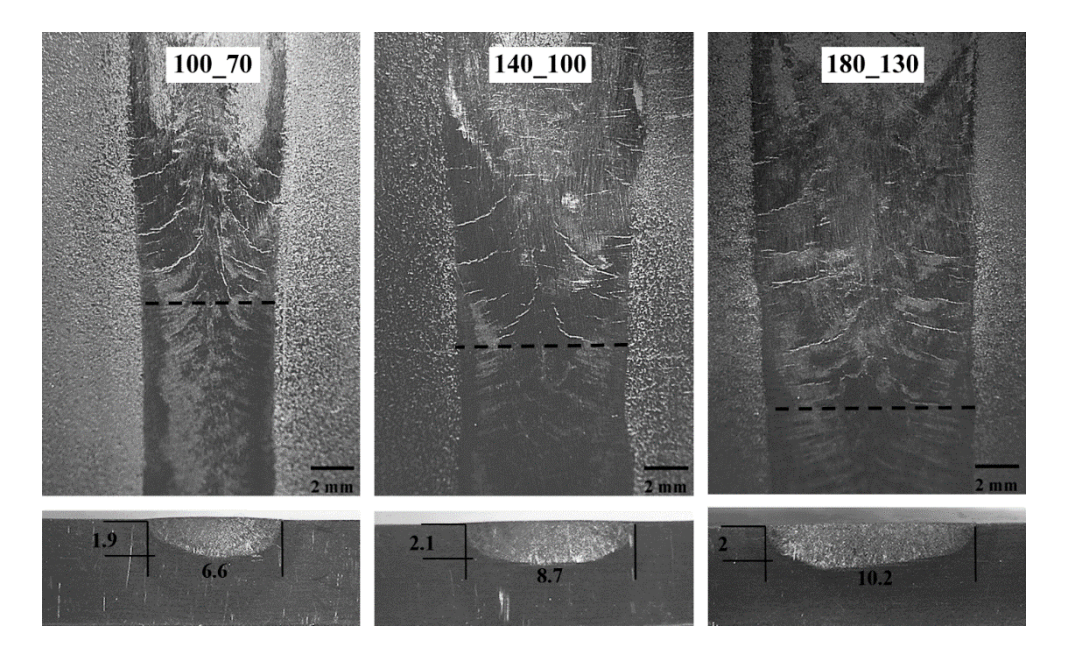


Figure 20. Top and transversal views of the welds including weld bead width and penetration values.

Hardness measurements are presented in Table 19. Similar values were found for both base metal and fusion zone of about 190 HV, while the heat affected zone (HAZ) exhibited a slightly lower value of  $170 \, \text{HV}$ .

Table 118. Average hardness values.

Base Metal	Heat Affected Zone	Fusion Zone
194±3	174±4	189±8

Table 20 represents the ferrite measurements in the base metal and weld metal. The weld length was divided into ten equidistant sections and ferrite measurements were done in each section from the start to the end of the weld. For each section it was also noted when cracking in the weld metal occurred. Average values in the base metal were 0.2 FN whereas the values in the weld metal varied between 0.2 and 1 FN.



Table 19. Ferrite number measurements in ten different positions of the weld metal and base metal

100_70	WM	BM	140_100	WM	BM	-	180_130	180_130 WM
Start	0.6	0.2	Start	0.4	0.2	-	Start	Start 0.3
	0.5	0.2		0.2	0.2			0.2
	0.2	0.2		0.2	0.2			0.2
	0.3	0.2		0.2	0.2			0.2
	0.2	0.2		0.2	0.2			0.3
	0.2	0.2		0.2	0.2		Crack	Crack 0.9
	0.2	0.1	Crack	0.2	0.2		Crack	Crack 1
Crack	0.3	0.2	Crack	0.4	0.2		Crack	Crack 0.9
Crack	0.5	0.2	Crack	0.4	0.2		Puddle	Puddle 3.4
Stop	0.6	0.1	Stop	2.6	0.2		Stop	Stop 3.7

The base metal exhibited a relatively low grain size of 20  $\mu$ m, as visible in Figure 21 a). In the HAZ grain growth occurred, reaching average value of 90  $\mu$ m, Figure 21 b).

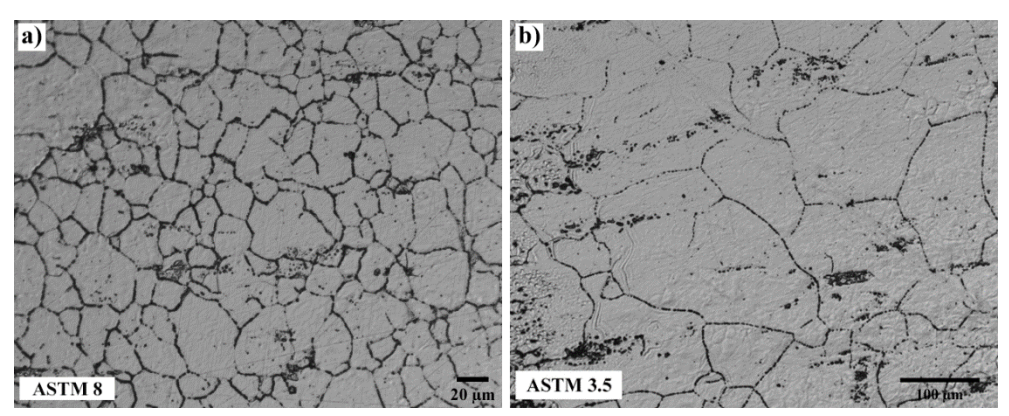


Figure 21. a) Base metal grain size, b) HAZ grain size.

Weld cracking under light optical microscopy from the 100\_70 is presented in Figure 22 a). A magnified image of the solidification crack is shown in Figure 22 b).

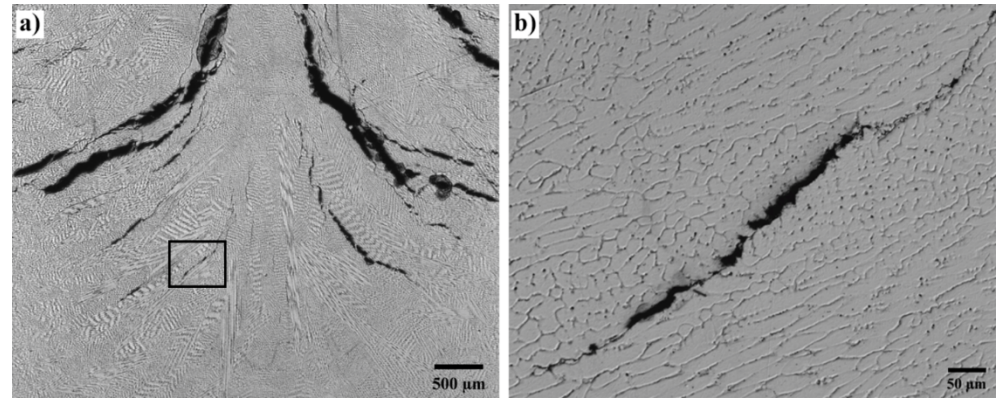


Figure 22. a) Light optical microscope image of solidification cracking, b) cracking occurring along solidification boundary.



# EXTRA TESTING OF AUSTENITIC STAINLESS STEEL

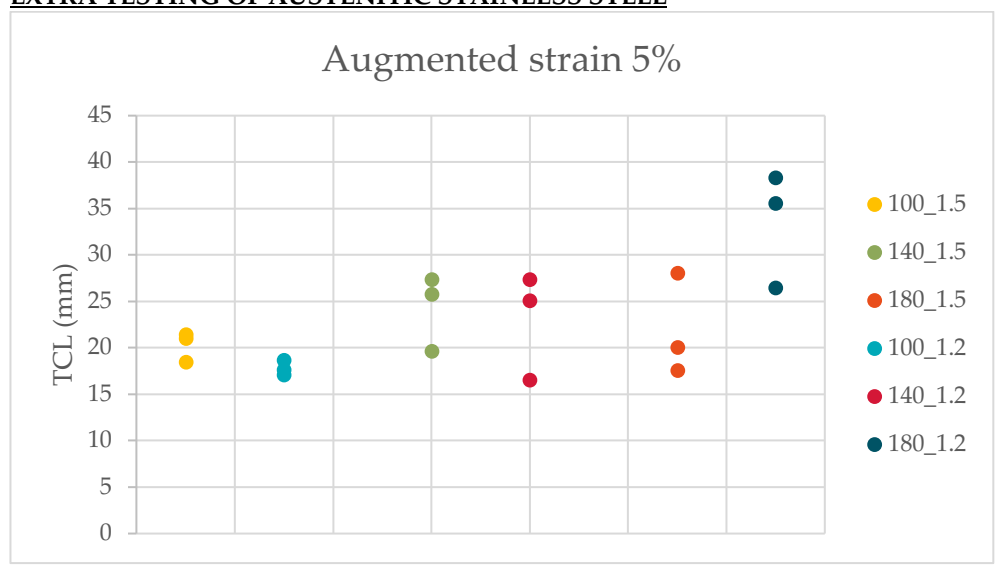


Figure 23. Solidification cracking response of austenitic stainless steel 314

Table 20. Welding parametres for the conditions in Figure 23

	100_1.5	140_1.5	180_1.5	100_1.2	140_1.2	180_1.2
A	98	137	175	98	137	175
V	10	13	12	9	12.7	13.8
mm/min	0.6	1.2	1.4	0.7	1.4	2
kj/mm	1.5	1.5	1.5	1.2	1.2	1.2



# 4 Analysis of the results

### 4.1 CAST ALLOY 718

The different grain structures in the weld metals suggests that thermal gradients were also different despite the welding conditions being the same. The example in Figure 1 from the as cast test plate, which showed more tortuous centreline with few equiaxed grains structure, is generally considered preferable in regards to cracking. On the other hand, the HIP conditions exhibited small cracks along the centreline grain. However, this behaviour was not consistent among the different test plates and the authors have no explanation for these anomalies. Moreover, as it can be noticed from Table 13, weld beads dimension/shape varied even though welding parameters and test conditions were the same. From the literature [13] it is known about the difficulty in obtaining good penetration when welding Alloy 718 due to the poor fluidity of the molten weld metal. Small variations of minor elements in Cast Alloy 718 are also known to promote differences in weld penetration [14]. Srinivasan et al. [15] have pointed out the high variability of TCL in relation to varying weld bead geometry during longitudinal Varestraint testing.

In general, the solidification cracking data from Figure 6 reveal the typical shape of Varestraint testing curves with increasing TCL until a saturation level is reached and there is no distinction in between the different conditions. The spread of Avg. TCL at 4% augmented strain can be related to both test and also to material associated scatter. A supporting fact that the three conditions behave similarly is related to the solidification range of the alloy which is dependent on the alloy composition [16]. As it is for the current study, the base metal compositions for the three conditions are the same, so is the solidification range, as it is an intrinsic property of the material. This confirms the hypothesis that the three conditions as cast, HIP-1120 and HIP-1190 have the same solidification cracking susceptibility. Such hypothesis is supported in a study conducted by Cieslak et al. [17], where a similar response in hot cracking susceptibility for two conditions of 625 Plus, aged and annealed, was found. Cieslak et al. assumed this to be related to the melting and solidification reactions occurring in the fusion zone, consequently eliminating the thermal history.

The cracking response in the HAZ follows a different trend in comparison to the FZ, Figure 7. As for the FZ crack measurements, the liquation cracking response discloses a significant amount of scatter. A possible explanation for the large spread in results when testing cast material can be related to the macrosegregation resulting from the casting process, which is not possible to eliminate completely even with the HIP treatments. Therefore, it is reasonable to expect such high variations in terms of cracking response, as the cracking behaviour of the material is dependent on local segregation condition in the cast plates especially when it comes to crack propagation properties.

The large scatter has been also reported also elsewhere in the literature [8] i.e. when conducting crack growth tests for cast Alloy 718. The same study also reflected on the high scatter for hot ductility tests. Moreover, studies regarding HAZ liquation cracking of Allvac® 718 Plus™ [18] in the wrought form, which is generally known to be more homogenized in terms of segregation, also revealed high variability from the crack measurements, with standard deviations overlapping between the different heat



treatment conditions. However, despite the large scatter as can be seen in Figure 7, the as cast condition exhibits the lowest cracking susceptibility at all strain levels but 3.2% augmented strain. The HIP-1120 and HIP-1190 show similar cracking response at low strain levels, but above 2.6% the HIP-1190 has the worst behaviour as represented with the highest Avg. TCL measurements.

In the as cast condition, small and interconnected liquation cracks were seen especially in areas where Laves phase have liquated. This could be a possible explanation for the lower Avg. TCL. Generally, they followed the solidification grain boundaries present from the casting process (dashed line in Figure 24), but few small cracks were also occurring intragranularly as indicated by the arrows. With increasing HIP temperature the amount of segregation decreased due to the dissolution of the secondary precipitates, the main effect being related to the reduction of the Laves content. This changed the cracking mechanism in the HIP conditions to grain boundary liquation mechanism as clearly visible in Figure 5. The cracks in the HIP-1120 and HIP-1190 conditions were surrounded by the presence of re-solidified products which suggests that liquid films along the grain boundaries existed prior to cracking. An explanation for this could be the enrichment of Nb from dissolution of secondary precipitates by diffusion mechanism which lowers the melting temperature. However, EDS linescans across the grain boundaries did not reveal any Nb enrichment. The reason could be that the resolution of the EDS could have been insufficient to investigate the microsegregation of Nb. Other than that, Huang et al. [19] have demonstrated by SIMS analysis the strong effect of B segregation at the grain boundaries on HAZ liquation cracking of cast Alloy 718. The higher Avg. TCL for the HIP-1190 can be related to the larger grain size for that HIP treatment. From Table 14, it can be noticed that by increasing the homogenization temperature, not only the volume fraction of the secondary precipitates changed, also, the grain size increased. HIP-1190 exhibited the highest value of 3.3 mm, almost twice in respect to the as cast with 1.7 mm, whereas the HIP-1120 had average grain size of 2.6 mm. Figure 24 also shows a relatively long and continuous crack along the grain boundary in the HIP-1190 condition. Note the "straightening" effect of the grain boundaries due to the increasing grain size in relation to the as cast, which had a more tortuous shape. Grain size is considered to be an important parameter when assessing the HAZ liquation cracking susceptibility. Generally, smaller grain size is believed to be beneficial in terms of resistance towards liquation cracking mainly because the larger grain boundary area allows a better strain accommodation [20]. Several studies investigating wrought and cast Alloy 718 [20–23] have agreed upon this, except of Huang et al. [24], who reported that micro cast heats with smaller grain size than the conventionally cast heats with larger grain size showed an increased cracking susceptibility, mainly due to the large amount of available liquation points.

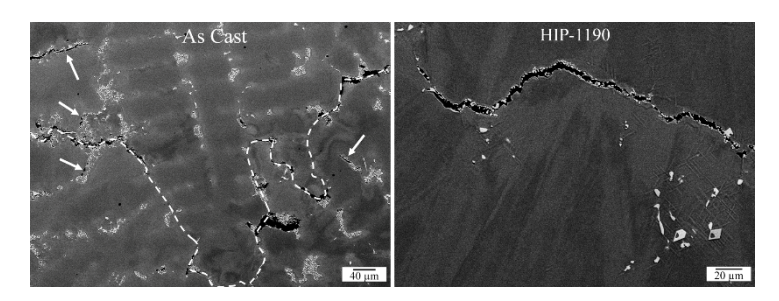


Figure 24. The picture on the left is showing HAZ liquation cracks in the as cast condition, the dashed line delineates the grain boundary and the arrows indicate locations where intergranular cracks occurred. On the right picture, liquation cracking in the HIP-1190 condition.



### 4.2 COMPARISON OF CAST ALLOY 718 AND 718 PLUS

Following figures compare heat affected zone cracking of Cast Alloy 718 and Cast Alloy 718 Plus in the as cast condition (Figure 25), after  $1120^{\circ}$ C/4h (Figure 26) and after  $1190^{\circ}$ C/4h (Figure 27).

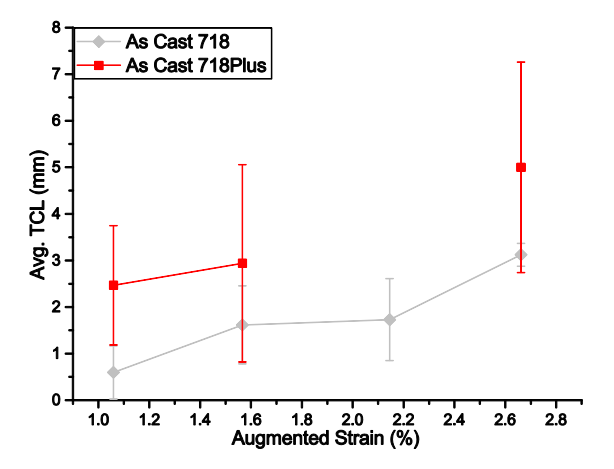


Figure 25. HAZ cracking in As Cast Alloy 718 and 718 Plus.

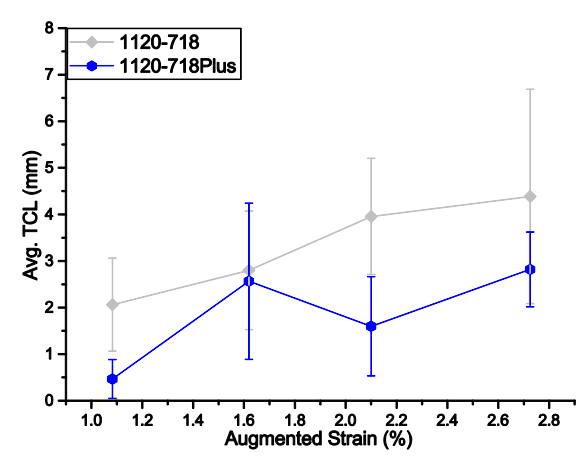


Figure 26. HAZ cracking in HIP-1120 (Cast Alloy 718) and Pseudo-HIP at 1120 (718 Plus).

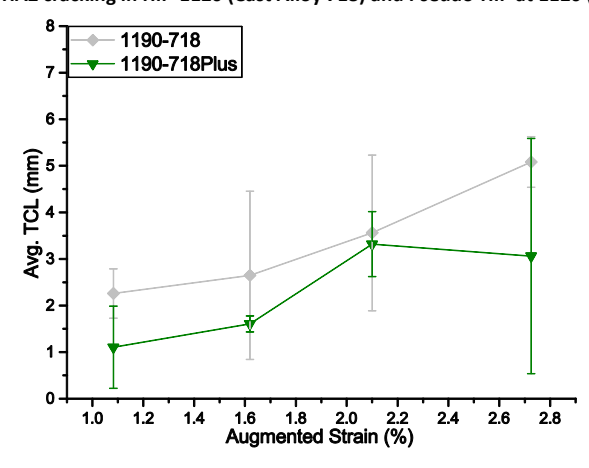


Figure 27. HAZ cracking in HIP-1190 (Cast Alloy 718) and Pseudo-HIP at 1190 (718 Plus).



It can be seen that as Cast 718Plus had higher cracking susceptibility than Cast Alloy 718, however, after heat treatments the cracking susceptibility of Cast 718 Plus decreased in relative to Cast Alloy 718.

The difference in cracking susceptibility was related to the combined effect of volume fraction of secondary precipitates, hardness and grain size. Their values are summarised and compared in Table 22.

Table 21. Comparison of volume fraction of secondary precipitates, grain size measurements and base metal hardness

	Cast 718 Plus			Cast 718		
	As Cast	1120°C/4h	1190°C/4h	As Cast	HIP-1120	HIP-1190
Vv (%)	3.2±1.8	0.7±0.6	0.2±0.1	3.7±0.6	1.7±0.1	1.3±0
HV	375±15	170±0	170±0	260±20	220±30	210±20
GS (mm)	2.3±0.5	2.2±0.5	1.7±0.4	1.7±0.1	2.6±0.3	3.3±0.3

### 4.3 WROUGHT 718 PLUS

The main effect of the longer dwell time heat treatment of  $950^{\circ}\text{C}/15$  h seems to provide more extensive amounts of precipitation with regard to eta phase in the microstructure as shown in Figure 12. The base metal hardness values suggest that the  $\gamma'/\gamma''$  precipitates are not fully dissolved [12]. The longer heat treatment for 15 h leading to coarsening of the  $\gamma'$  may be an explanation to the reduced hardness of about 340 HV, in comparison to about 380 HV for the 950°C/1 h condition. However, it is difficult to say whether eta phase precipitation has any effect on hardness or not. Base metal grain size of 8.3  $\mu$ m (950°C/1 h) and 7.8  $\mu$ m (950°C/15 h) indicates that the longer heat-treatment time did not result in grain growth. However, comparison of Figures 5 and 7 and results from Table 3 shows that the larger fraction of eta phase precipitates is effective in pinning the grain boundaries in the HAZ of 950°C/15 h. Average grain size in the HAZ resulted to be about 9.6  $\mu$ m in comparison to 950°C/1 h condition, which exhibited significant grain growth, about 30  $\mu$ m in average grain size.

Two main liquation mechanisms were seen to occur: grain boundary liquation and constitutional liquation of NbC. Cracking connected to the highly liquated regions was associated with constituents having eutectic morphology, often associated with Nb-rich  $\gamma$ /Laves eutectic. The delta/eta phase is generally known to aid liquation by two mechanisms, constitutional liquation [13], [14] and Nb enrichment on grain boundaries through solid state dissolution [6], [15], [16]. However, it is difficult to conclude about the governing mechanism in the current study, since the characterization would require the use of more advanced analysis techniques. Moreover, in 950°C/15 h condition (Figure 18), further away from the fusion line, cracks were free from any visible liquation products. EDS linescan analyses did not reveal any Nb enrichment in this area. Cracks were surrounded by thick and round edged eta precipitates, which is indication of the initial steps of dissolution [6]. Precipitates with similar characteristics are reported to have a dual role in regards to grain boundary properties: grain boundary pinning and embrittlement effect. Andersson et al. [4] have reported a higher hardness of 50 HV for



950°C/15 h than 950°C/1 h condition after on-heating quenching tests conducted by Gleeble testing at temperatures up to 1150°C. A shift of ductility curve to lower values was observed for the 950°C/15 h condition in the same temperature range, below the nilductility temperature. Keeping the above considerations in mind, grain boundary embrittlement may explain the cracking occurring in the region where partial dissolution of eta phase occurs.

### 4.4 AUSTENITIC STAINLESS STEEL 314

The welds of austenitic stainless steel 314 fall in the fully austenitic mode according to the WRC-1992 diagram [5]. The very low Creq/Nieq of 1.14, where Creq=Cr+Mo+0.7Nb=24.72 and Nieq=Ni+35C+20N+0.25Cu=21.64, makes it highly susceptible to solidification cracking according to the Lippold et al. [6]. Ferrite measurements in the weld metal confirm the fully austenitic mode in the welds, the variations in Table 10 are believed to be in the general error range. It should also be noted that the ferrite measurements in the weld metal may not truly reflect the ferrite content due to the low penetration of the welds.

From the results it can be seen that varying amperage and welding speed by maintaining the same input, the amount of cracking changed. The cracking seems to be related to the depth to width ratio of the weldments: from Figure 20 it can be seen that the depth remained the same but the width increased with increasing amperage and welding speed, which led to difference in depth to width ratios (D/W). Moreover, as the D/W decreased, the cracking started in earlier stage in relation to higher D/W, as it can be seen from the dashed lines in the same figure and the crack locations in the first columns of Table 10. The D/W for 100\_70, 140\_100 and 180\_30 are, respectively, 0.29, 0.24 and 0.20 It should be noted that there is not a large variation in D/W. Generally, it is preferred to have depth to width ratio of 1:1. Moreover, it was interesting to see the larger scatter in

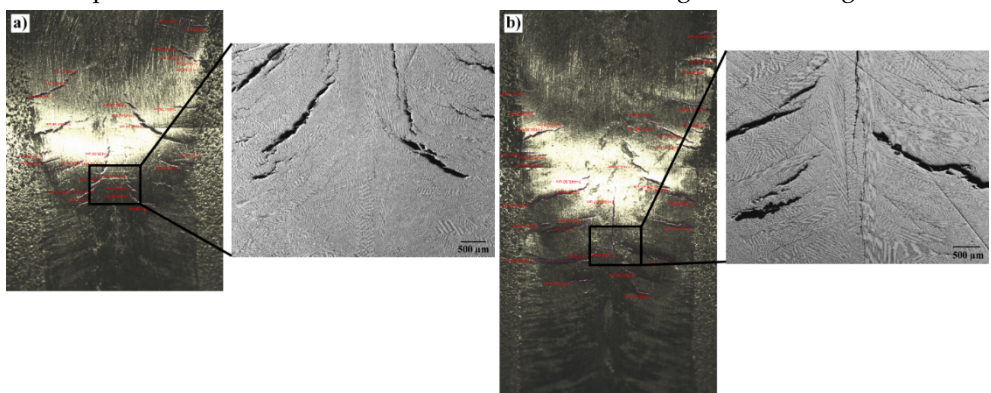


Figure 28. Test plates from the welding parameter of 140\_100 a) with the lowest cracking, b) with the highest cracking

cracking for the 140\_100 test condition. Figure 28 shows the different cracking locations in the two test plates, with lowest cracking of 23 mm and the largest 41 mm. These two test plates in Figure 28 a) and b) resemble those of 100\_70 and 180\_30 in Figure 4. To note also the similarities in the crack locations and morphologies, in Figure 28 a) cracking occurring in the region of maximum bending of the plate, in Figure 28 b) the cracking started in an earlier stage. Therefore, the large test scatter in the 140\_100 was due to the change in the cracking location.

KME

34

# 5 Conclusions

### 5.1 CAST ALLOY 718

The results indicate no difference relative to the solidification cracking susceptibility between the three conditions.

The susceptibility towards HAZ liquation cracking can be ranked as follows: HIP-1190 having the highest susceptibility, followed by HIP-1120 and the as cast having the lowest cracking susceptibility. In the current study it was found that especially the amount of secondary precipitates and base metal grain size seem to have a significant role in determining susceptibility towards the HAZ liquation cracking.

### 5.2 CAST 718 PLUS AND COMAPRISON WITH CAST ALLOY 718

No difference in cracking was seen in between the Pseudo-HIP treatments at 4h. Higher cracking susceptibility was observed for conditions heat treated at 24h. The as cast condition had higher cracking susceptibility in relatevily to the as cast condition of Cast Alloy 718. However, after HIP-1120 and HIP.-1190 of Cast Alloy 718 had higher cracking susceptibility than that of Pseudo-HIP 1120 and 1190 of Cast 718 Plus. Combined effects of volume fraction of precipitates, grain size and hardness were seen to influence the cracking susceptibility.

### 5.3 WROUGHT 718 PLUS

The important effect of the higher amount of eta phase precipitation at 950°C/15 h can be summarized as follows:

- it limits the grain growth by grain boundary pinning in the HAZ;
- it contributes to extensive liquation;
- it increases hot cracking susceptibility

### 5.4 AUSTENITIC STAINLESS STEEL 314

It was seen that the welding parameter set 100\_70, with 100 A and 70 mm/s, the lowest values among the test parameters, also produced the least amount of solidification cracking in the weld metal with a minimum amount of variation.



### 5.5 SUMMARY

Overall, the investigation concerning Ni-based superalloys shows that the cracking susceptibility in the fusion zone (solidifcation cracking) is not influenced by the different heat treatments. Regarding the cracking susceptibility in the heat affected zone (liquation cracking), it is seen that the cracking behavior is affected by the heat treatment. Generally, increasing the heat treatment temperature and the soak time the cracking behaviour deteriorated which was attributed to the effect of volume fraction of secondary precipitates, grain size and hardness. Welding parametres play an important role on the solidification cracking of austentic stainless steels. Low speed and amperage are found to have the least amount of cracking in the weldments.

As can be seen from the project results, weldability cracking is a general phenomenon that must be tackled to create good fabrication control independed of alloy system. All alloys investigated have in common that they are austenitic alloys, although the actual microstructural phenomena behind may differ. Formation of un-wanted pahses and the precise control of welding parameters are shown to be of paramount importance. It should be noted that e.g. formation of reaction products involved in the cracking may have different kinetics for different materials and hence it is not possible to set-up same recommendations for different materials, the important aspect is rather that there is basic fundament in terms of weld cracking that needs to be understood and based on this the proper procedures can be settled.



# 6 Goal fulfilment

The overall goal was to get a beetter knowledge of the hot cracking phenomena and provide testing data to the industrial partners. The previously mentioned goals are considered to be fulfilled:

- To accomplish a licentiate engineer
   The student has accomplished the Licentiate degree in May
- 2) To develop a unified theory for hot cracking In consideration to an unified theory the effect of welding parametres, volume fraction of secondary precipitates, grain size and hardness have to be included
- 3) To develop a testing rationale for hot cracking
- 4) To generate weldability test data on materials relevant to the boiler industry Weldability test data is provided for austenitic stainless steel 314 in the report
- 5) To recommend materials and parametres for improved weldability

  Literature review on hot cracking in austentic stainless steels and weldability
  test data for both austenitic steel (314) and Ni-based superalloys (Cast 718,
  718Plus and wrought 718Plus) is provided
- 6) To establish a testing methodology that can be used for assessing weldability with respect to hot cracking susceptibility



# 7 Suggestions for future research work

The project disclosed a number of interesting findings with regard to hot cracking in both gas turbine as well as boiler materials and has contributed to closing some research gaps. However, it is highly recommended to continue the research on hot cracking on the above metioned material groups in order to provide more insight on how to avoid or minimizing hot cracking in already existing as well as newly developed (i.e. Haynes 282) hard-to-weld-materials. It is also suggested to couple the research that has been performed in KME 719 to be coupled with more advanced characterization such as TEM.



# **8** Literature references

- [1] J. Jacobsson and J. Andersson, Weldability of Superalloy Alloy 718 and ATI® 718Plus™ A study performed with Varestraint Testing, Mater. Test., vol. 59.9, pp. 769–773, 2017.
- [2] *GORDINE, J. Some problems in welding Inconel 718*, Weld. Res. Suppl., vol. 50, no. 11, p. 480–484s, 1971.
- [3] SPICER, R.A.; BAESLACK III, W.A.; KELLY, T.J. Elemental effects on GTA spot weld penetration in Cast Alloy 718, Weld. Res. Suppl., p. 285–288s, 1990.
- [4] SRINIVASAN, G.; BHADURI, A.K.; SHANKAR, V.; RAJ, B. Evaluation of hot cracking susceptibility of some austenitic stainless steels and a nickel-base alloy, Weld. World, vol. 52, no. 7–8, pp. 4–17, 2008.
- [5] PUMPHREY, W. I.; JENNINGS, P. H. A consideration of the nature of brittleness at temperatures above the solidus in castings and welds in aluminium alloys. Journal of the Institute of Metals, 1948, 75.4: 235-&.
- [6] CIESLAK, M. J.; HEADLEY, T. J.; FRANK, R. B. The welding metallurgy of custom age 625 PLUS alloy. Welding Journal, 1989, 68.12: 473-482.
- [7] BARRON, M. L. Crack Growth-Based Predictive Methodology for the Maintenance of the Structural Integrity of Repaired and Nonrepaired Aging Engine Stationary Components. GE AIRCRAFT ENGINES CINCINNATI OH, 1999.
- [8] VISHWAKARMA, K.; CHATURVEDI, M. A Study of HAZ Microfissuring in a Newly Developed Allvac 718 Plus Superalloy, in Superalloy 2008, 2008, pp. 241–250.
- [9] HUANG, X.; CHATURVEDI, M.C.; RICHARDS, N.L. Effect of homogenization heat treatment on the microstructure and heat-affected zone microfissuring in welded cast alloy 718, Metall. Mater. Trans. A, vol. 27, no. 3, pp. 785–790, 1996.
- [10] DUPONT, J.N.; LIPPOLD, J.C.; KISER, S.D. Welding metallurgy and weldability of nickel-base alloys. Hoboken, N.J.: John Wiley & Sons, 2009.
- [11] THOMPSON, R. G.;CASSIMUS, J. J.; MAYO, D. E.; DOBBS, J. R.; The relationship between grain size and microfissuring in alloy 718. Welding journal, 1985, 64.4: 91-96.
- [12] HONG, J.K.; PARK, J.H.; PARK, N.K.; EOM, I.S.; KIM, M.B.; KANG, C.Y. Microstructures and mechanical properties of Inconel 718 welds by CO2 laser welding, J. Mater. Process. Technol., vol. 201, no. 1–3, pp. 515–520, May 2008.
- [13] WOO, I.; NISHIMOTO, K.; TANAKA, K.; SHIRAI, M. Effect of grain size on heat affected zone cracking susceptibility. Study of weldability of Inconel 718 cast alloy (2nd Report). Welding international, 2000, 14.7: 514-522.
- [14] HUANG, X.; RICHARDS, N. L.; CHATURVEDI, M. C. Effect of grain size on the weldability of cast alloy 718. Materials and Manufacturing Processes, 2004, 19.2: 285-311.
- [15] D. J. Kotecki and T. A. Siewert, WRC-1992 constitution diagram for stainless steel weld metals: a modification of the WRC-1988 diagram, Weld. J., vol. 71, no. 5, pp. 171–178, 1992.
- [16] J. C. Lippold and D. J. Kotecki, *Welding Metallurgy and Weldability of Stainless Steels*. John Wiley & Sons, 2005.



# 9 Publications

SINGH, Sukhdeep; ANDERSSON, Joel. Review of Hot Cracking Phenomena in Austenitic Stainless Steels. In: 7th International Swedish Production Symposium, SPS16, Lund, Sweden, October 25–27, 2016. Swedish Production Academy, 2016. p. 1-7.

SINGH, Sukhdeep; ANDERSSON, Joel. Hot cracking in cast alloy 718. Science and Technology of Welding and Joining, 2018, 1-7.

SINGH, Sukhdeep; ANDERSSON, Joel. Hot cracking in cast 718 Plus and comparison with cast Alloy 718. In Manuscript.

SINGH, Sukhdeep; ANDERSSON, Joel. Preliminary investigation on effect of welding parametres on solidification cracking of austenitic stainless steel 314, Submitted.

SINGH, Sukhdeep; ANDERSSON, Joel. Varestraint weldability testing of ATI 718Plus - Influence of eta phase. To be presented at Superalloy 718 and Derivates Conference 2018.



# DEVELOPMENT OF WELDABILITY ASSESSMENT AND UNDERSTANDING OF HOT CRACKING IN BOILER AND GAS TURBINE MATERIALS

The aim of the project was to bring an improved understanding of weldability with a specific focus on hot cracking of alloys used in temperature applications. The alloys investigated were austenitic stainless steel 314, which is being used in the boiler industry, as well as Ni-based superalloys such as the cast Alloy 718, wrought and cast ATI 718Plus which are being used in aeroengine applications. A state-of-the art Varestraint weldability test method, developed during a previous KME research project, has been used for testing in the current project.

It was found that the pre-weld heat treatment condition significantly influences the hot cracking susceptibility of the Ni-based superalloys. Generally, by increasing heat treatment temperature and the soak time, the extent of the cracking increased in the weld heat affected zone. Moreover, testing of the austentic stainless steel showed that the welding parametres also play an important role relative to the cracking and the scatter of the results.

The report includes the weldability testing data for the different alloys together with report of the general microstructure of the base metal, heat treatments and welded zones with an overview of the main factors influencing the cracking susceptibility.

Energiforsk is the Swedish Energy Research Centre – an industrially owned body dedicated to meeting the common energy challenges faced by industries, authorities and society. Our vision is to be hub of Swedish energy research and our mission is to make the world of energy smarter. www.energiforsk.se

